JOURNAL OF OPTOELECTRONICS AND ADVANCED MATERIALS Vol. 10, No. 3, March 2008, p. 639 - 644

A study of patch antennas on ZST substrate

O. G. AVĂDANEI, A. IOACHIM[a,*], P. GASNER, G. N. PASCARIU, V. PASCARIU
"Al. I. Cuza" University of Iaşi, Romania
[a]INFIM Bucharest, Romania

Compactness of microstrip antennas has made them very attractive for applications in communication systems. As the need for antenna miniaturization continues, a possible solution is offered by the utilization of high dielectric constant materials as substrate. The purpose of this paper is the study of patch antennas on high permittivity dielectric substrates $(Zr_{0.8}\ Sn_{0.2})TiO_4$ – ZST. A comparative investigation of different types of patch and arrays was performed Two substrate thickness h_1=1 mm and h_2=2 mm at a frequency of f=1090 MHz was considered. The main advantage of ZST material as a dielectric substrate for patch antennas is the miniaturization of the antennas as well as a high stability with the temperature. For each case we presented the radiation pattern, the efficiency and the input impedance of the patch antennas. The patch antennas were designed using an improved cavity model (a further improved Richards cavity model). The radiation pattern for rectangular array with n = 4, 16, 32 are also presented. The numbers are imposed by the feeding system of the array, which must ensure the same phase for all the patches. A discussion on the suitability of patch antennas with high permittivity substrate is done.

(Received September 25, 2007; accepted March 12, 2008)

Keywords: High permittivity dielectrics, Patch antennas, Input impedance, Radiation pattern, Antenna array

1. Introduction

The rapid development of the communication infrastructure, occured in the last period of time, has imposed a constant research effort in developing of new materials, microsystems and microstructures which would alow for a more advanced degree of miniaturization, and a better stability with temperature. The main requirement for miniaturization of the components is the high dielectric permittivity of the material, but this is not the only requirement for a material with application in communication devices. It is also necessary a low dielectric loss to enssure a better efficiency of the device in our case of the patch antenna, and o good stability with the temperature to enssure a better frequency stability of the antenna.

The ZST dielectric made by us shows a high permittivity, ε=36, a very low dielectric loss coefficient tanδ = 0.0004, and a very good stability with the temperature. This material was synthesized by conventional solid-state methods from individual high-purity oxide powders (>99.9%). The starting materials were mixed according to the desired stoichiometry of $(Zr_{0.8},\ Sn_{0.2})TiO_4$ ceramics, with a 2 wt % La_2O_3 and 1 wt % ZnO additions as a sintering aid. The powders were ground in distilled water for 24 h in a mill with agate balls. All the mixtures were dried and treated at 1200 ^oC for 2h. The calcined powders with 0.2 wt% NiO addition were then remilled for 2h with PVA solution as a binder. Substrate plates were formed by uniaxial pressing and sintered at temperatures of (1330-1400) ^oC for (2-4)h.

The morphology, phase-composition and microstructure observation of the sintered ceramics were performed by means of scanning electron microscopy (SEM), and energy-disperse X-ray spectrometry (EDX). The crystalline phases were identified by X-ray diffraction (XRD).

The dielectric permittivity (ε_r) and the quality factor values (Q) at microwave frequencies were measured using the Hakki-Coleman dielectric resonator method.

The advantages and drawbacks of patch antennas with high permittivity substrate are still controversial, and some interesting results were reported in [1], [2], [3], [4].

For our study we have chosen a rectangular patch antenna. The rectangular patch antenna and the coordinate system for the cavity are shown in Fig. 1. Such an antenna can be excited by a microstrip line or by a coaxial line. Taking into account the fact that the dielectric substrate is brittle, the microstrip line feed solution is the only one acceptable for the moment. The design of this microstrip patch antenna was made using an improved cavity model [5] which is a further developed Richards cavity model [7].

The Cavity Model made by Lo [6] and improved by Richards [7] is based on the following considerations:

a) The electric field $\vec{E}$ has only *z* component and the magnetic field $\vec{H}$ has only *xy*-components in the region bounded by the microstrip and ground plane.

b) The fields are independent of the *z*-coordinate for all frequencies of interest.

c) All the walls along the edges are perfect magnetic walls. In consequence there are no tangent components of the magnetic field $\vec{H}$ along the edge.

In conclusion this model treats the antenna as a cavity bounded by electric walls above and below, and magnetic walls along the edges.

One of the most important drawbacks of the cavity model was the fact that first it supposes the cavity perfect, and calculate the fields inside it, and then with this fields are calculated the radiation currents at the sides walls. In

our model [5] we have suppose that the fields extend outside the cavity, that the magnetic walls are not perfect and the magnetic field amplitude along the x axis has the variation presented in Fig. 2. The resonant frequency of a patch with the length *a* is the same as that of a cavity with the length *a+2dl,* where [8]

$$dl = 0.412h\frac{(\varepsilon_{eff} + 0.3)(b/h + 0.264)}{(\varepsilon_{eff} - 0.258)(b/h + 0.8)} \quad (1)$$

and ε_{eff} is the dielectric permittivity for a microstrip, considered as a transmission line.

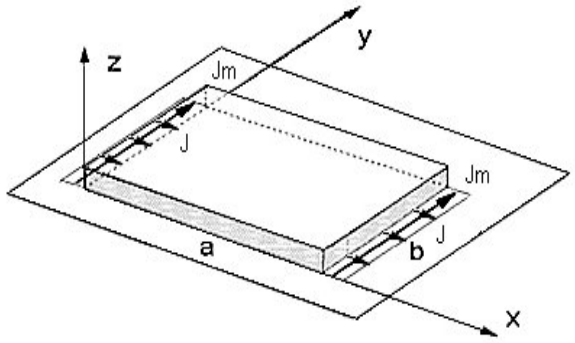

Fig. 1. The representation of radiating currents.

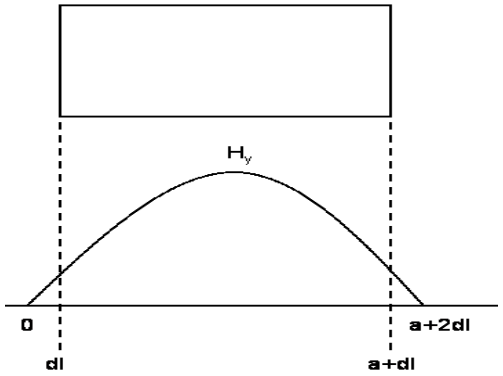

Fig. 2. The representation of the magnetic field H_y along x axis.

For this reason we have assumed that the fields are extending outside the patch on a distance *dl*, and the patch act as a cavity with the length *a+2dl*. In this case, if the excited mode is TM_{100}, the fields inside the antenna are [5]:

$$E_z = E_0\cos(\pi x/(a+2dl)) \quad (2)$$

$$H_y = \frac{j\omega\varepsilon}{\pi}aE_0\sin(\pi x/(a+2dl))$$

and the length of the patch would be taken between *dl* and *a+dl*. In this case the magnetic field is zero at the coordinate *0* and *a+2dl* but it would not be zero at the ends of the patch: *dl* and *a+dl*. This means that besides the magnetic currents generated by E_z at the borders there will be also electric currents *J* generated by H_y. In this approximation the radiating currents on the side walls are [5]:

$$\vec{J}_{my} = E_z\hat{z}\times\hat{x} = E_0\cos\frac{\pi dl}{a+2dl}\hat{y} \quad \text{for } x = dl \text{ and } x = a+dl \quad (3)$$

$$\vec{J}_z = \hat{x}\times H_y\hat{y} = \mp H_0\sin\frac{\pi dl}{a+2dl}\hat{z} \quad \text{for } x = dl \text{ and } x = a+dl \quad (4)$$

After the rotation of the radiating apertures in a position parallel to the ground plane the relation (4) would become:

$$\vec{J}_x = H_0\sin\frac{\pi dl}{a+2dl}\hat{z} \quad \text{for } x = dl \text{ and } x = a+dl \quad (5)$$

With those radiating currents: two electric, and two magnetic currents situated above the ground plane the radiated fields of the patch antenna are [5]:

$$E_\theta = -\frac{jk}{\pi r}\exp(-jk_0 r)E_z\cdot\int_0^h\int_{-b/2}^{b/2}e^{(jk_0 y\sin\theta\sin\phi)}\cos\left(\frac{jk_0 a\sin\theta\cos\phi}{2}\right)dydh\cos\phi - $$

$$-\frac{j\omega\mu_0}{\pi r}\exp(-jk_0 r)H_y\int_0^h\int_{-b/2}^{b/2}e^{(jk_0 y\sin\theta\sin\phi)}\cos\left(\frac{jk_0 a\sin\theta\cos\phi}{2}\right)dydh\cos\theta\cos\phi \quad (6)$$

$$E_\phi = -\frac{jk}{\pi r}\exp(-jk_0 r)E_z\cdot\int_0^h\int_{-b/2}^{b/2}e^{(jk_0 y\sin\theta\sin\phi)}\cos\left(\frac{jk_0 a\sin\theta\cos\phi}{2}\right)dydh\sin\phi\cos\theta - $$

$$-\frac{j\omega\mu_0}{\pi r}\exp(-jk_0 r)H_y\int_0^h\int_{-b/2}^{b/2}e^{(jk_0 y\sin\theta\sin\phi)}\cos\left(\frac{jk_0 a\sin\theta\cos\phi}{2}\right)dydh\sin\phi \quad (7)$$

In the equations (6) and (7) we have take into account the ground plane, k_0 is the wave number in free space and the two cosines terms under the integration represent the array factor for the two magnetic currents. From these relations we can determine the radiated fields until a constant E_0 that depend of the excitation conditions.

To assure an efficient feeding of the antenna it is necessary to obtain a proper impedance matching between the antenna and the microstrip feeding line. To achieve this goal it is necessary to predict the input impedance of the antenna as a function of the feeding point position. The input impedance is calculated by the following relation [8], [9]:

$$\frac{1}{R_{mn}} = \frac{\mu_0 hc^2}{\varepsilon_r \omega_{mn} \delta_{eff}} \psi_{mn}^2(x_0, y_0) G_{mn} \qquad (8)$$

where $$G_{mn} = \frac{\sin(n\pi d_x / 2a)}{n\pi d_x / 2a} \cdot \frac{\sin(m\pi d_y / 2b)}{m\pi d_y / 2b}$$

and $$\psi_{mn} = \frac{\chi_{mn}}{\sqrt{ab}} \cos k_n x \cos k_m y$$

The factor G_{mn} accounts for the width of the feed, χ_{mn} is a normation factor, c is the speed of light, and δ_{eff} is an effective loss tangent in witch are included also the losses in metallic walls and the radiating losses. For microstrip feed patch antennas the effective feed dimensions (d_x, d_y) are taken equals to the physical dimensions of the microstrip line.

For our antenna the power dissipated in dielectric P_d is [9]

$$P_d = \delta\omega\varepsilon \int_{dl}^{a+dl} \int_0^b \int_0^h \vec{E} \cdot \vec{E}^* dv \qquad (9)$$

And the losses in the electric conducting walls P_m are given by the relation

$$P_m = 2\sqrt{\frac{\omega\mu}{2\sigma}} \int_{dl}^{a+dl} \int_0^b \vec{H} \cdot \vec{H}^* dS \qquad (10)$$

For an antenna array the radiation pattern is found by multiplying the array factor with the radiating pattern of one element. The array factor for planar array with m elements on x-coordinate and n elements on y-coordinate is given by [8]:

$$E = E_p \sum_{s=1}^{m} \exp(j(s-1)(\delta + kdx \sin\theta\cos\varphi)) \sum_{s=1}^{n} \exp(j(s-1)(\delta + kdy \sin\theta\sin\varphi)) \qquad (11)$$

where δ is the faze factor between two consecutive elements and dx, dy are the distances between two consecutive elements along the x respective y axes; E_p is the field radiated by a patch.

2. Computed results

For our study we have designed two types of patch antennas, with two different substrate thickness h_1=2 mm, h_2=1 mm, at the same resonant frequency 1090 MHz. The geometrical dimensions for the first antenna are: a_1=22.6 mm, b_1=38 mm, and for the second: a_2=22.9 mm, b_2=38 mm. We have chosen the width of the antennas greater then the length because the radiated power of a patch antenna is in direct proportionality with b^2. The only problem in this case is that the feeding point must be on the middle of the antenna width to avoid the excitation of the TM_{010} and TM_{110} modes.

In Fig. 3 we present the dependence of the real part of the input impedance with the position of the feeding point for both antennas. The position of the feed point, which enssure the best impedance match at the microstrip feed line, for the antenna with h_1=2 mm thickness is x_1 = 9 mm and y_1 = 19 mm. For the antenna with h_2=1 mm thickness this point is x_2 =8.3 mm, y_2 = 19 mm.

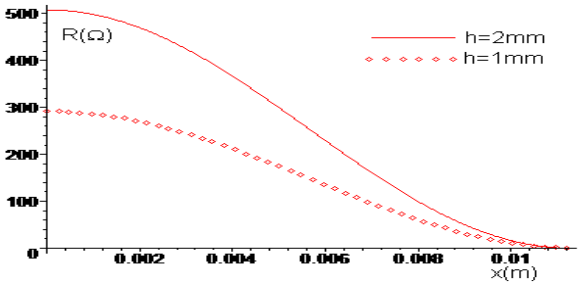

Fig. 3. The dependence of the input impedance with feeding point.

The normalized power radiation patterns of the two antennas in the φ=0 plane and φ=90^0 are shown in Fig. 4a and Fig. 4b. From these images it is clear that the antenna with 2 mm substrate thickness would radiate more than five times power comparatively with the 1 mm thickness antenna.

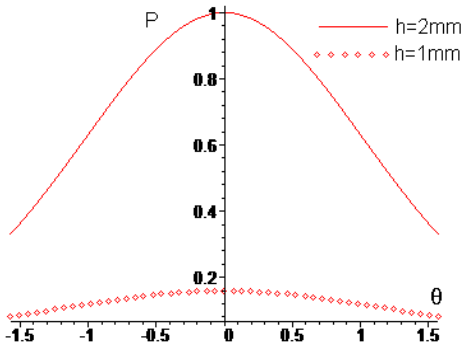

Fig. 4a. Radiation pattern for φ=0.

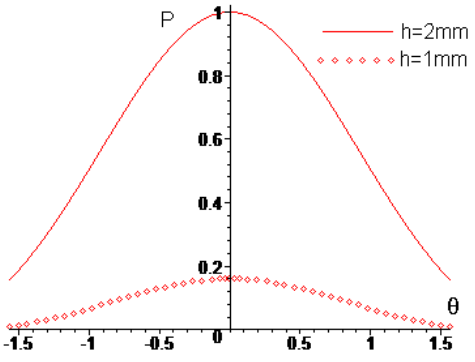

Fig. 4b. Radiation pattern for φ=90°.

An antenna with high permittivity substrate is considerably smaller than other antenna. On the other hand, patch antenna are very often used in antenna array and usually the distance between elements is taken $\lambda_0/2$. However, high permittivity antenna can be placed at considerably smaller distances then $\lambda_0/2$. For this reason we have made a study of different types of antennas array with 4 (2×2), 16 (4x4) and 32 (8×4) elements situated at a distance of $\lambda_0/2$ or $\lambda_0/4$. θ

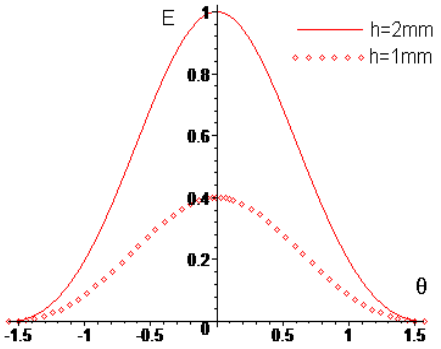

Fig. 5a.

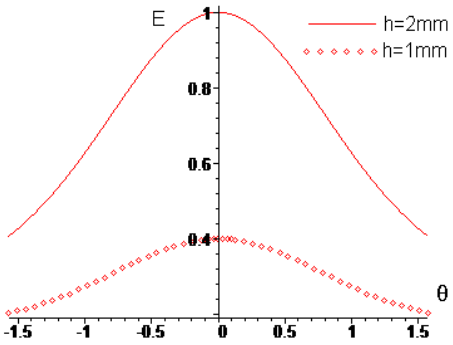

Fig. 5b.

In Fig. 5a and 5b we present the normalized field radiation pattern for a 4 elements antenna array, in the plan φ=0, for a distance between elements $d_1 = \lambda_0/2$ and respectively $d_2 = \lambda_0/4$.

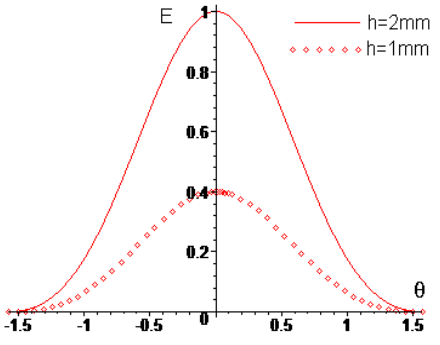

Fig. 6a.

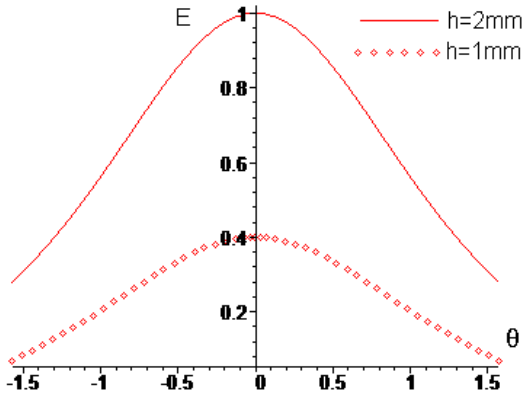

Fig. 6b.

In Fig. 6a and 6b we present the normalized field radiation pattern for a 4 elements antenna array, in the plan φ=90°, for a distance between elements $d_1 = \lambda_0/2$ and respectively $d_2 = \lambda_0/4$.

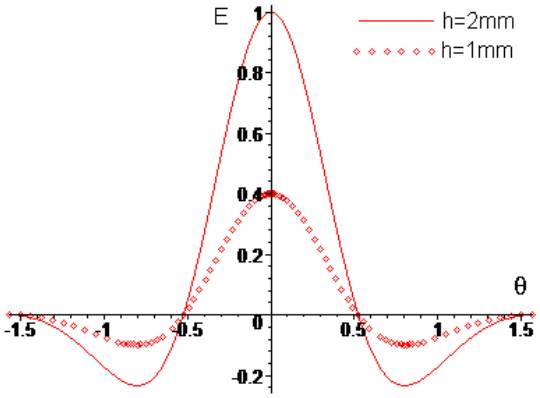

Fig. 7a.

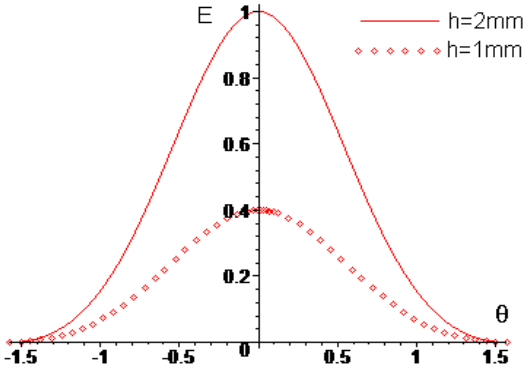

Fig. 7b.

In Fig. 7a and 7b are present the normalized field radiation pattern for a 16 elements antenna array, in the plan φ=0, for a distance between elements $d_1 = \lambda_0/2$ and respectively $d_2 = \lambda_0/4$.

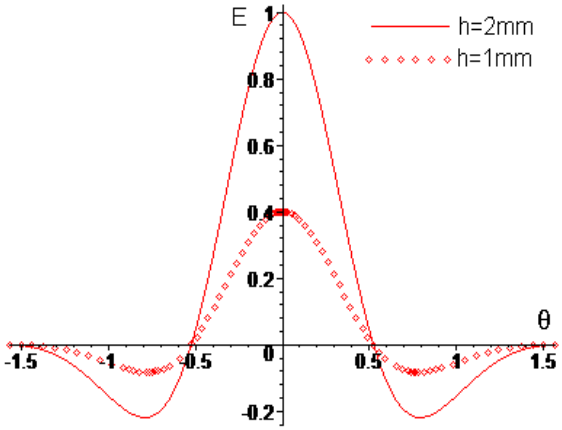

Fig. 8a.

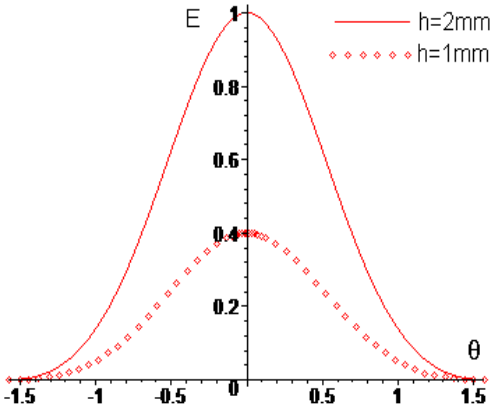

Fig. 8b.

In Fig. 8a and 8b are shown the normalized field radiation pattern for a 16 elements antenna array, in the plan φ=90°, for a distance between elements $d_1 = \lambda_0/2$ and respectively $d_2 = \lambda_0/4$.

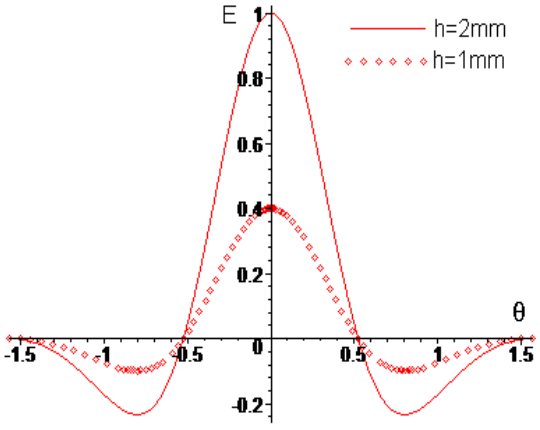

Fig. 9a.

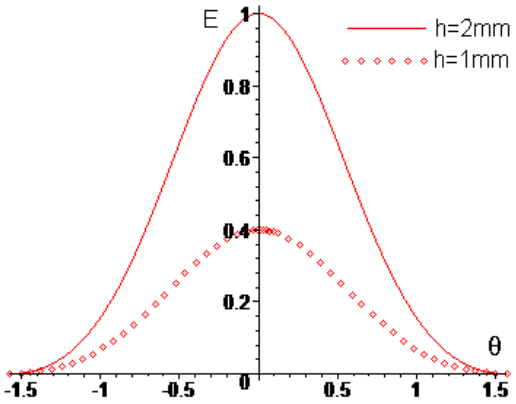

Fig. 9b.

In Fig. 9a and 9b are shoen the normalized field radiation pattern for a 32 elements antenna array, in the plan φ=0, for a distance between elements $d_1 = \lambda_0/2$ and $d_2 = \lambda_0/4$, respectively.

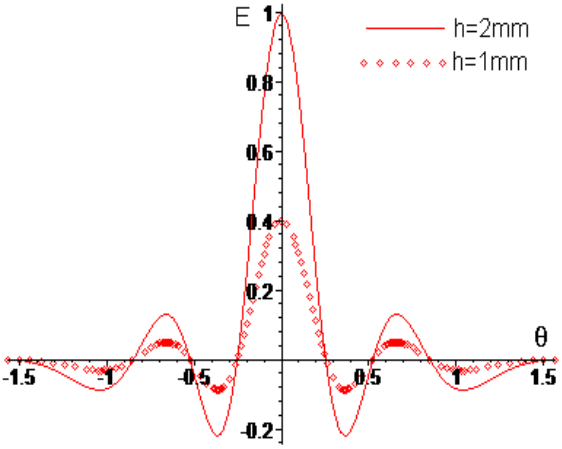

Fig. 10 a.

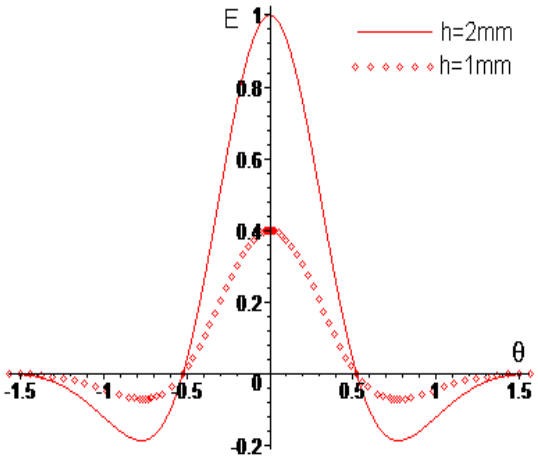

Fig. 10 b.

In Fig. 10a and 10b are present the normalized field radiation pattern for a 32 elements antenna array, in the plan φ=90°, for a distance between elements $d_1 = \lambda_0/2$ and respectively $d_2 = \lambda_0/4$.

The field distribution pattern of the radiated fields in a plan, parallel with the antenna, situated at 10m distance, for the 32 elements array, with a distance $d_1 = \lambda_0/2$ between elements is presented in Fig. 11. A similar field distribution pattern for the 32 elements array with a distance $d_2 = \lambda_0/4$ between elements is presented in Fig. 12.

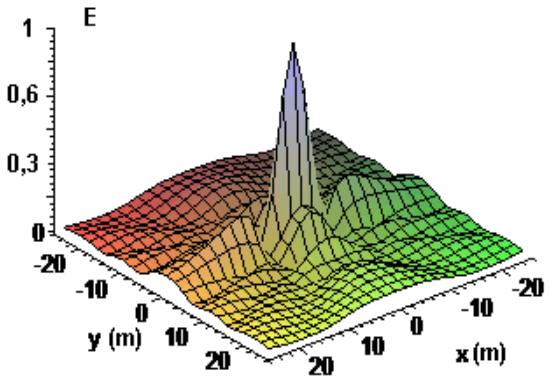

Fig. 11.

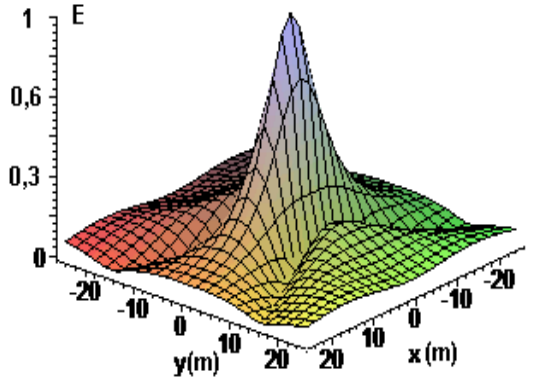

Fig. 12.

3. Conclusions

The ZST $(Zr_{0.8}, Sn_{0.2})TiO_4$ ceramic material allowed for an important reduction of the patch antenna dimensions which is an very interesting feature. The material high hardness allowed only the microstrip line feed solution.

The patch antenna length *a* is the dimension that determine the radiation frequency. The antenna width *b* has a great influence on the radiated power and a small influence to the radiation frequency and to the input impedance. The width *b* was chosen greater than the length to increase the power radiated by the antenna.

From Fig. 3 we can see that the input impedance has its maximum value at the wall of the antenna and zero at the center. Also we can see that for the 2 mm thick antenna the impedance matching with the microstrip line is harder to obtain. However, at 1090 MHz, the input impedance around the feeding point has a variation of 4Ω/0.1 mm for the 2 mm thick antenna and around 3 Ω/ 0.1 mm for the 1 mm thick antenna, which are reasonable values for both antennas.

From Fig. 4 and Fig. 5 it is obvious that the 2mm thick antenna has a significant greater output power, comparatively the 1mm antenna. Also the yields of the two antennas are: 81% for the 2 mm antenna and only 51% for the 1mm antenna. The losses in the metallic walls are the most important losses that occurs in a ZST patch antenna. The microstip line for 2 mm thick antenna is significantly wider, $w_1 = 0.47$ mm, comparatively with the microstrip line for the 1mm thick antenna where $w_2 = 0.17$ mm, and so much easier to manufacture. From those data it is clear that the 2 mm thick antenna is considerably more efficient.

The power radiated by an antenna array depends mainly on the element number. The $\lambda_0/2$ antennas arrays have a better directivity then the $\lambda_0/4$ arrays. The only advantage of the $\lambda_0/4$ arrays is the fact that they have a smaller number of side lobes. For example, the 16 elements $\lambda_0/2$ array has two side lobes when the 16 elements array $\lambda_0/4$ has none. The 32 elements $\lambda_0/2$ array has six side lobes in the φ=90° plan while the 32 elements array $\lambda_0/4$ has only two.

References

[1] T. K. Lo, Electronic Letters **33**, 9-10 (1997).
[2] J. S. Colburn, Y. Rahmat-Samii, IEEE Antennas. Propag. **47**(12), 1785-1794 (1999).
[3] Sung-Hun Sim, Chong-Yun Kang, Ji-Won Choi, Seok-Jin Yoon, Hyun-Jai Kim, Young-Joong Yoon, Journal of Materials Science: Materials in electronics, **13**, 207-211 (2002).
[4] D. D. Sandu, O. G. Avădănei, A. Ioachim, D. Ionesi, J. Optoelectron. Adv. Mater. **5**(5), 1381-1387 (2003).
[5] D. Sandu, O. G. Avădănei, A. Ioachim, G. Banciu, P. Gasner**,** J. Optoelectron. Adv. Mater. **8**(1), 339-344 (2006).
[6] Y. T. Lo, D. Solomon, W. F. Richards, IEEE Trans. Antennas Propagation. AP-**27**, 137-145 (1979).
[7] W. F. Richards, Y. T. Lo, D. Harrison, A.P-**29**, 38-46 (1981).
[8] N. Balanis "Antenna theory: Analysis and design", sec. edition, John Wiley&Sons, N.Y. 1997, chapter 14.
[9] W. F. Richards, Y. T. Lo, Fellow, J. Brewer IEEE Trans. Antennas Propagation AP-**29**, 150-151 (1981).

*Corresponding author: ioachim@infim.ro